Open Access Research Journal of
Engineering and Technology
Journals home page: https://oarjpublication/journals/oarjet/
ISSN: 2783-0128 (Online)

OARJ OPEN ACCESS RESEARCH JOURNALS

(RESEARCH ARTICLE)

Check for updates

Energy Recovery from LNG (Part 1): Techno-economic assessment of the retrofit of an existing LNG regasification facility with an organic rankine cycle for power production

Raphael Gregory Rauceo *

Not affiliated, Siparia, Trinidad and Tobago.

Open Access Research Journal of Engineering and Technology, 2026, 10(01), 062-076

Publication history: Received on 09 February 2026; revised on 16 March 2026; accepted on 18 March 2026

Article DOI: https://doi.org/10.53022/oarjet.2026.10.1.0023

Abstract

Research in the area of LNG cold energy offers the opportunity to maximize the gain of this cold energy. Therefore, this article examines the feasibility of the Propane Organic Rankine Cycle (ORC) and explores how to maximize the gain from this cycle. This article analyses Key Performance Metrics (KPMs) versus process parameters. DWSIM was used to simulate the cycle using the Peng Robinson 1978 Advanced thermodynamics model and the economics and heat exchanger calculations were performed using Python in DWSIM. It is shown that the new KPMs, Total Annualized Earnings (TAE) and Annualized Interest Rate of Return (AIRR) for the base case are USD300.5k and 14 % and for the alternative case, the TAE and AIRR are USD857.1k and 23.4 %. The net power extracted per unit mass of LNG for each case is 0.0084 kWh/kg and 0.0097 kWh/kg respectively. Therefore, this ORC is feasible. It is also shown that reducing the LNG pressure results in a greater TAE. The TAE and AIRR for this cycle are USD535.9k and 18.5 %, an over 75 % TAE increase compared to the base case which makes it more profitable than the base case.

Keywords: ORC; LNG; Cold Energy Use; Techno-Economic Assessment (TEA); Exergy Analysis; Sensitivity Analysis

1. Introduction

Natural gas is an important fuel for energy production and is also used in the manufacture of chemicals and plastics. The share of natural gas in the global energy supply is 23 % [1]. The world saw around 550 bcm of liquified natural gas being exported in 2024 which was just under 15 % of natural gas consumption [2]. Liquefied Natural Gas (LNG) supply is set to rise by 7 % or 40 bcm in 2026 [3] Oil major Shell forecasts a rise in global demand for LNG by around 60 % by 2040 [4]. The cold energy of LNG is a valuable source of energy. This energy can be used to produce work. The exergy of LNG calculated at -161 ^{o}C and 1.13 bar at reference conditions of 27 ^{o}C and 1.01 bar is 1051.8 kJ/kg or 0.292 kWh/kg. This is the maximum thermodynamic work that can be obtained from the LNG from bringing it from the aforementioned conditions to atmospheric conditions.

There are some conventional technologies for vaporizing LNG where the energy is released to the air or seawater. They are listed below:

- Open Rack Vaporizers (ORV) [5]: Heat is exchanged between a falling film of ambient seawater and the LNG in an open rack finned panel type arrangement. The seawater temperature is typically above 5 ^{o}C to prevent freezing [6]. A large flow of water is required for a large flow of LNG. The main cost of regasification of the LNG is the cost associated with pumping of the seawater. The thermal impact of the ejected seawater on the quality of water and marine life is the major concern.
- Submerged Combustion Vaporizers (SCV) [5]: The Boil off Gas is burned in the combustion burner. The flue gas is used to heat a water bath where LNG flows through a stainless-steel tube submerged in a water bath. The high thermal capacity of the bath permits more operational control for stable operation of the process

* Corresponding author: Raphael Rauceo

- Intermediate Fluid Vaporizer (IFV)) [7]: IFVs are compact heat exchangers that consists of three sections: 1) A condenser that transfers the latent energy of the intermediate fluid (IF) to LNG, 2) An evaporator that vaporizes the IF 3) A gas heater as a heat source [8] [9]. Typically, the evaporator and the condenser are contained in the shell of the IFV while the gas heater is separate from the shell.

One of the problems with this process is the temperature of the water which pose a risk to the quality of the marine ecosystem. Warmwater species will not reproduce at temperatures below 20 ^{o}C while tropical species will die at temperatures of 10 ^{o}C to 20 ^{o}C [10]. Several authors have reviewed the uses of cold energy. Some of the uses are listed below.

There are numerous technical articles on the utilization of LNG cold energy Some of the ways this cold energy can be utilized are [11] [12] [13]: 1) For power generation with the Rankine cycle, Brayton cycle and the Kalina cycle, 2) air separation, 3) desalination of seawater, 4) CO_2 capture, 5) data center cooling, 6) storage of cold energy and 7) food processing and improving of the operating performance of equipment.

Electrical power generation is one of the most flexible ways to utilize LNG cold exergy since electrical power can be used industrially, commercially and in domestic households. ORCs & Natural Gas Direct Expansion are utilized to generate power from LNG cold exergy [14]. ORCs have been pervasively employed in industry for industrial waste heat recovery [15], from geothermal energy sources [16] , from biomass energy sources [17] and high pressure natural gas expansion. The installed capacity of ORCs in 2017 was 2.7 GW with 460 MW of new capacity being announced or in building phase [18]. This cold energy can be usefully employed instead of wasting it to the environment.

Putra et al[19] analyzed the electricity generation process using the Direct Expansion, Rankine cycle and the combined Direct Expansion and Rankine cycle for the Gresik LNG receiving terminal with a natural gas regasification rate of 60.95 MMSCFD. They performed simulation of the processes using UNISIM and economic analysis of the processes using the publication by A M Gerrard [20]. They found that the Direct Expansion scheme was the only feasible one with a positive NPV. It had a NPV of $USD 695, 032.

The above article provides valuable information into the use of the cold energy of LNG for power generation and the evaluation of the different technologies that use the cold energy of LNG.

There are several process parameters that requires evaluation in a single stage ORC including the fluid composition for the cycle which is an important parameter for cycle optimization [21]. It is not analyzed in this article. Critically examining these parameters will lead to a better understanding of the economic design and operation of the cold energy ORC. The following parameters are examined in this article 1) LNG heat exchanger and vaporizer outlet temperature difference, 2) Pump and turboexpander efficiency, 3) Turboexpander inlet pressure, 4) Electricity cost and interest rate and their effect on KPMs are examined to determine the feasibility of the cycle. These KPMs are introduced later in this article.

Therefore, this article presents the use of DWSIM for the simulation and modelling of a single stage propane ORC without heat integration using an inherently safer design (i.e. Stainless Steel). Asia imports a lot of LNG hence a retrofit of a hypothetical facility in Thailand is examined in this article. The objective of this article is to present the findings of the feasibility and sensitivity analysis of the ORC using the KPMs, to present new ways of evaluating the information and to provide recommendations for further analysis of the process and optimization. This work is motivated by the need for alternative energy sources, reduction of carbon emissions and the study of the design, analysis and optimization of processes.

2. Methodology

2.1. Introduction

DWSIM V9.0.2 was used to simulate the cycle. Heat exchanger modelling and economic modelling were also performed. The Peng-Robinson 1978 (PR78) Advanced equation of state was employed. CoolPack V1.5 and Symmetry (trial version) were employed to verify the thermodynamic properties of the fluids and the process simulation. The cycle contained: 1) a heat exchanger for the condensation of propane using LNG, 2) a pump for increasing the pressure of the liquid propane, 3) a vaporizer for vaporizing the propane stream and 4) a turboexpander for producing electricity. A PFD of the cycle is shown in
Figure 1.

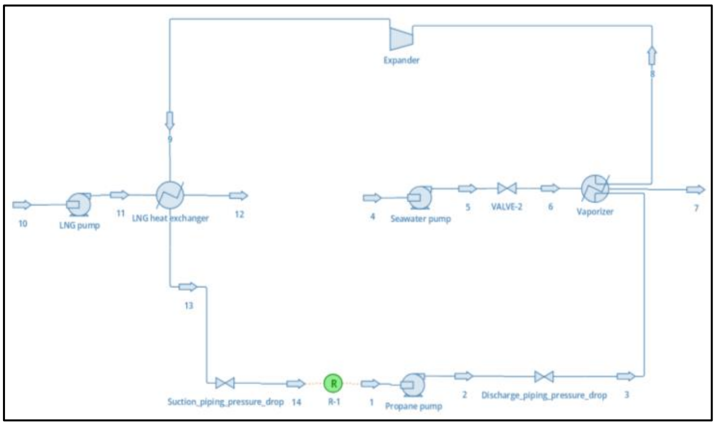

Figure 1 Process Flow Diagram of the ORC

Plate and frame heat exchangers were employed in the design to achieve low minimum approach temperatures in the heat exchangers. The costing for the brazed aluminum heat exchanger was not available.

2.2. Process Design Basis

The design basis for ambient conditions and the process design basis are shown in Table 1 and Table 2 respectively.

Table 1 Ambient Conditions **[22]**

Parameter	**Value**
Minimum temperature	299 K
Maximum temperature	309 K
Pressure	101325Pa

Table 2 Process Design Basis **[13] [10] [23] [24] [25] [26] [27]**

LNG:	
Composition:	
Methane	96.48 %
Ethane	1.96 %
Propane	0.36 %
n-Butane	0.07 %
i-Butane	0.09%
Nitrogen	1.04 %
Mass flowrate	22.9 kg/s
Propane mass flowrate	22.0 kg/s
Seawater mass flowrate	504.4 kg/s
Turbo-machinery:	
Pump efficiency	80 %
Turboexpander efficiency	90 %
Generator efficiency	98%

Turboexpander inlet pressure	400 kPa_g
LNG pressure exit pump	7 MPa_g
Heat Exchangers:	
Heat exchanger minimum approach temperature	2 K
Minimum discharge seawater temperature	293 K
Cryogenic heat exchanger:	
Pressure drop (LNG side)	70 kPa_g
Pressure drop (Propane side)	50 kPa_g
Overall HTC	6000 W/m^2 K
Vaporizer:	
Pressure drop (seawater side)	100 kPa_g
Pressure drop (Propane side)	50 kPa_g
Pump suction pressure	34 kPa_g
Overall HTC	5000 W/m^2 K
Maintenance days	10 days / year
Facility life	20 years
Pump suction and discharge piping pressure drop	5 kPa_g

The reference conditions for the calculations were 300 K and 101325 Pa. An efficiency equation was developed for the pump motors using the information from Towler et al [28].

2.3. Assumptions and Risks

Some of the assumptions and technology risks considered in the calculations are listed below. It was assumed that:

1) The 2 exchangers could be purchased. The associated risk was due to the pressure difference in the LNG heat exchanger while there was a probability of ice forming in the vaporizer.
2) The existing facility LNG vaporizer and the seawater pump wouldn't be reused.
3) Only 4 additional operators were required.
4) The cost was for a new facility due to the size and complexity of the project compared to the existing facility
5) The location factor for the plant was not applicable
6) Stainless steel was conservatively employed in the calculations for the cycle.

2.4. Economics Model and Key Performance Metrics

Towler et al [28] have the following equation to calculate the cost of each equipment:

$$C_e = a + bS^n \quad \text{Equation 1}$$

Where S is a size factor, a,b,n are equipment cost constants and C_e is the equipment cost.

Turton et al [29] have the following cost equation for the turboexpander:

$$log_{10}C_p^o = K_1 + K_2 log_{10}(A) + K_3[log_{10}(\mathrm{A})]^2 \quad \text{Equation 2}$$

Where A is the size factor, K_{1-3} are equipment cost constants and C_p^o is the equipment cost

Tammone [30] has the following equation for the generator cost, C_{eg}, referenced at November 2014 prices where W_g is the generator power in kW varying between 80 kW and 10 MW. The gearbox cost is 40 % of the generator's cost [31].

$$C_{eg} = \frac{578.4}{567.3}\left[10^{\substack{4.105466+0.057044log_{10}W_g+\cdots \\ 0.079664(log_{10}W_g)^2}}\right] \quad \text{Equation 3}$$

After the cost of the equipment was calculated from the equipment size, the cost at the required date, June 2024, was calculated using Chemical engineering cost indices [31]. The cost index in June 2024 was 798.8.

Using the equipment costs, the cost of a greenfield facility was calculated for the process based on the equipment cost calculation from Towler et al [28] and Turton et al [29]. The production cost (PC) was calculated using the maintenance and insurance cost (5% factor), operator cost, direct salary overhead cost (60 % factor) and plant overhead cost using the information from Towler et al [28]. The contingency factor was not included in the equation from Turton et al.

The financial data below are based on information from Thailand.

Table 3 Key financial data

Parameter	Value
Price of power [32]	6.06 Baht per kWh
Exchange rate [33]	33 Baht per 1 USD
Interest rate [34]	6.5 %

Several key performance metrics are examined against the process parameters. The Annualized Fixed Capital Investment (AFCI) was calculated [35] and from this cost and the product cost the TAE were calculated. Net power is sold. The yearly salary of a process operator in Thailand was USD12,892 [36].

Yearly earnings = Yearly revenue – AFCI – PC Equation 4

The AIRR was also calculated. This is the rate that is required to set the Yearly Earnings to zero.

Key technical performance metrics were also calculated to evaluate the cycle [37]. The Cycle Electrical Energy Efficiency (CEEE) was calculated to evaluate the efficiency in converting the energy added to the cycle to electrical energy.

$$CEEE = \left(\frac{W_g}{\Delta H_{vap} + W_{PL}}\right) * 100 \qquad \text{Equation 5}$$

The Cycle Exergy Utilization Efficiency (CEUE) is a measure of how efficient the cycle is in converting cycle exergy (maximum work potential of the cycle) into useful work [13] [38].

$$CEUE = \left(\frac{W_G}{\Delta B_{Wi} + \Delta B_{Li} + W_p - \Delta B_{Wo} - \Delta B_{Lo}}\right) * 100 \qquad \text{Equation 6}$$

The Cycle Exergy Recuperation Ratio is the maximum work the cycle can achieve to the exergy input into the cycle.

$$CERR = \left(\frac{\Delta B_{Wi} + \Delta B_{Li} + W_p - \Delta B_{Wo} - \Delta B_{Lo}}{\Delta B_{Wi} + \Delta B_{Li} + W_p}\right) * 100 \qquad \text{Equation 7}$$

The ratio of the exergy destroyed to the exergy loss shows the exergy lost in the process versus the exergy leaving the process that can be used in a downstream process or cycle. Where ΔB is the change in exergy referenced to ambient conditions. The subscripts g, vap, p, i, o, w, l signify generator, vaporizer, pump, input and output stream, water and LNG respectively.

A lot of exergy is destroyed in heat exchangers. A new parameter called the Temperature Difference Ratio is a measure of exergy destruction in a heat exchanger at a specified minimum approach temperature (i.e. economic ΔT_{min}) due to the mismatch of the hot and cold streams and can be used for optimization of this match.

$$TDR_{\Delta T_{min}} = \frac{\Delta T_{min}}{\Delta T_{LMTDa}} \qquad \text{Equation 8}$$

Propane was analyzed in this study.

This study examines the variation of each parameter of the cycle and examines the effect each parameter has on key dependent variables. This will allow for the better design of these cycles. The base case and its alternative are first examined.

3. Discussion

3.1. Base Case

The results of the base case design are summarized in Table 4 & 5.

Table 4 Key Financial Results Summary

Metric	Value
Yearly earnings	USD300.5k
Annualized interest rate of return	14 %

Table 5 Key Technical Results Summary

Metric	Value
Power produced	941.5 kW
Cycle electrical energy efficiency	5.87 %
Cycle exergy efficiency	3.81 %
Cycle exergy utilization efficiency	9.7 %
Cycle exergy recuperation ratio	0.4
Ratio of exergy destroyed / loss	0.6
Temperature difference ratio, TDR_{2^oC}(LNG heat exchanger)	0.097
Temperature difference ratio, TDR_{2^oC} (vaporizer)	0.072
Power produced per mass of LNG	0.0084 kWh kg^{-1}

The yearly earnings and the AIRR are USD300.5k and 14 % respectively. The yearly earnings are a positive number and the AIRR is more than the project interest rate. Therefore, the project is feasible using this case. The installed cost of the two heat exchangers is approximately 3 % of the equipment installed cost. 5.87 % of the energy input into the cycle are converted to electrical power. 3.81 % of the maximum work potential of the input streams are converted to electrical power. 9.7 % of the potential maximum work of the cycle is produced in electrical power. The cycle reduces the work potential of the input streams by 40 % and the ratio of exergy destroyed to loss is 60 % meaning most of the exergy is lost in the outlet streams. TDR_{2^oC} for the LNG heat exchanger and for the vaporizer are 0.097 and 0.072. These values mean that there isn't a good match in the temperature profile between the hot and cold streams in each heat exchanger and this results in a large destruction of exergy. Therefore, the cycle extracts a small part of the energy from the energy inputted but it is still feasible. The net power produced per mass of LNG is 0.0084 kWhkg^{-1}. This value is much lower than the actual exergy value of the LNG.

Figure **2** gives a breakdown of the exergy destroyed and lost in the cycle.

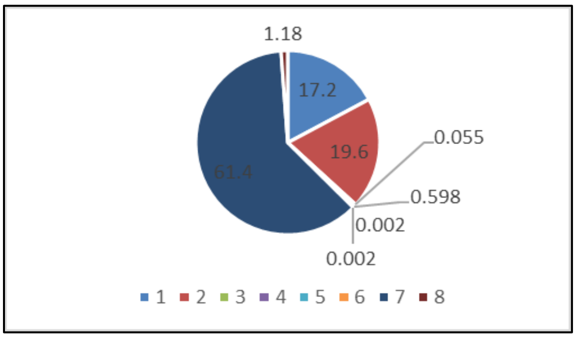

Figure 2 Exergy Destruction and Loss Diagram (Base Case, Total Value = 23.4 MW)

Table 6 Exergy Diagram Legend

1	LNG heat exchanger	5	Pipe 1 exergy loss
2	Vaporizer	6	Pipe 2 exergy loss
3	LNG pump	7	LNG stream out
4	Turbo-expander	8	Water stream out

Figure **2** shows how the exergy is distributed in different parts of the cycle. Most of the cold exergy is lost in the LNG leaving the cycle. A lot of the cold exergy is destroyed in the heat exchangers.

3.2. Alternative Case

The alternative case to the base case examines the cycle with 10 K sub-cooling to the inlet of the pump. The 10 K of sub-cooling allowed for further increases in the mass flowrate of the working fluid. The mass flowrate was increased to a maximum of 32.4 kgs^{-1} with a resultant increase in power to a value of 1.39 MW. The results of the alternative case are summarized in Table 7 and Table 8:

Table 7 Key Financial Results Summary

Metric	**Value**
Yearly earnings	USD 857.1k
Annualized interest rate of return	23.4 %

Table 8 Key Technical Results Summary

Metric	**Value**
Power produced	1.39 MW
Cycle electrical energy efficiency	8.15 %
Cycle exergy efficiency	5.68 %
Cycle exergy utilization efficiency	14.1 %
Cycle exergy recuperation ratio	0.402
Ratio of exergy destroyed / loss	0.576
Temperature difference ratio, TDR_{2^oC} (LNG heat exchanger)	0.108
Temperature difference ratio, TDR_{2^oC} (vaporizer)	0.099
Power produced per mass of LNG	0.0097 kWh kg^{-1}

The financial indicators for the project indicate that the project is feasible. The yearly earnings and the AIRR are USD 857.1k and 23.4 % respectively. The yearly earnings are a positive number and the AIRR is more than the project interest rate. The alternative case has higher yearly earnings and AIRR than the base case which means it is more profitable than the base case.

8.15 % of the energy input into the cycle are converted to electrical power. 5.68 % of the maximum work potential of the input streams are converted to electrical power. 14.1 % of the potential maximum work of the cycle is produced in electrical power. The cycle reduces the work potential of the input streams by 40.2 % and the ratio of exergy destroyed to loss is 60 % meaning a large part of the exergy is lost in the outlet streams. The TDR_{2^oC} for the LNG heat exchanger and for the vaporizer are 0.108 and 0.099 respectively. These numbers are better than the numbers from the base case indicating a better match between the hot and cold streams at the same minimum temperature. The power produced per mass of LNG is 0.0097 kWhkg^{-1}. *Figure 3* gives a breakdown of the exergy destroyed and lost in the cycle.

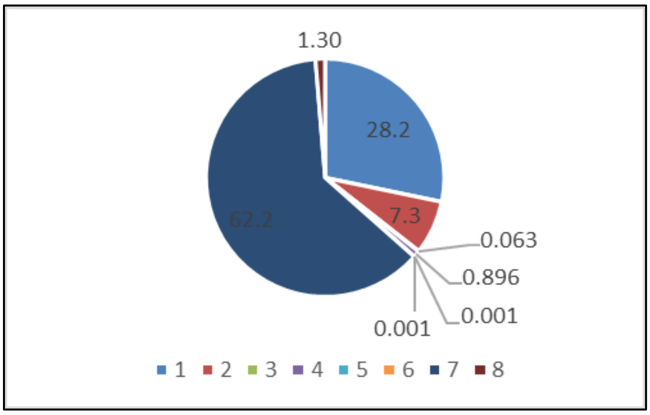

Figure 3 Exergy Destruction and Loss Diagram (Alternate Case, Total Value =23 MW)

Most of the cold exergy in *Figure 3* is lost in the LNG leaving the cycle. Less cold exergy is destroyed while the quality of the outlet stream is reduced compared to the base case. A large part of the exergy destroyed shifts from the vaporizer to the LNG heat exchanger. The increase in temperature difference between the hot and cold streams allowed for the optimization of the mass flowrate of the working fluid. In contrast, the base case design allows for the implementation of several cycles to extract power from the cold energy and for reducing the exergy destroyed in the heat exchangers. Optimization can still be performed on them

3.3. Sensitivity Analysis of the Base Case

3.3.1. LNG Heat Exchanger Outlet Temperature Difference

This section analyzes the outlet temperature difference at the exit of the LNG heat exchanger which is also the degree of sub-cooling at the inlet of the propane pump. This is represented on the x-axis as the temperature difference between the hot and cold streams at the outlet of the heat exchanger where 1 K of sub-cooling of the working fluid at the suction of the pump gives a 121.1 K temperature difference at the outlet of the LNG heat exchanger and an increase of the degree of sub-cooling causes an equivalent decrease in the temperature difference between the hot and cold streams at the outlet of the same heat exchanger.

The AFCI decreases as the temperature difference increases and the duty of the LNG heat exchanger decreases as it has the greater effect on the AFCI. Figure 4 shows the TAE at a propane mass flowrate of 22 kgs^{-1}. The trend at a mass flowrate of 16.7 kgs^{-1} is the same and is not shown.

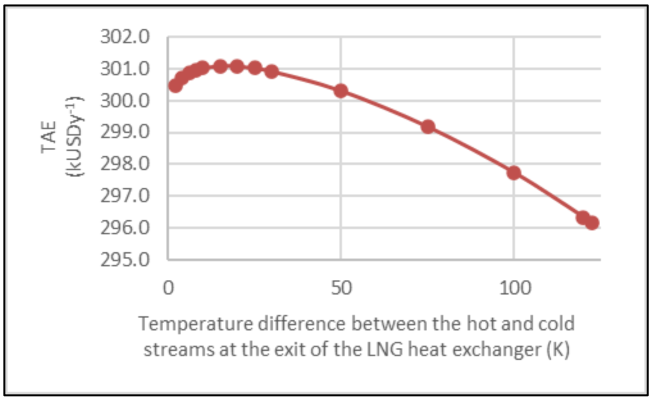

Figure 4 TAE vs Mass Flowrate (22 kgs^{-1})

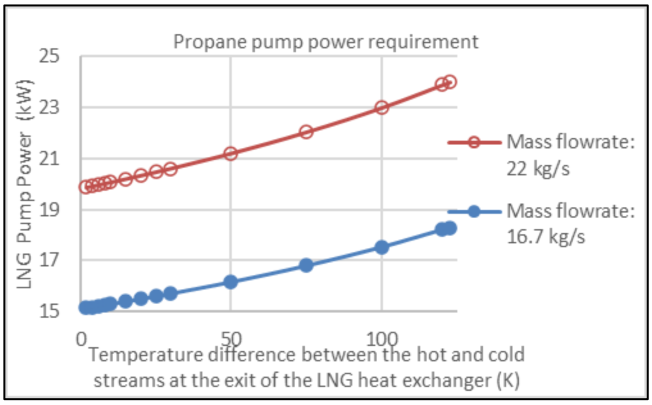

Figure 5 LNG Pump Power Required vs LNG Heat Exchanger Outlet Temperature Difference (Mass Flowrate: 22 kgs^{-1} and 16.7 kgs^{-1})

The TAE increases as the LNG heat exchanger outlet temperature difference increases. It then decreases. The operating cost increases as the volumetric flowrate of the fluid increases and hence pump power requirement increases. The rate of decrease of each is different resulting in a maximum TAE of USD301.1k. Figure 5 shows that sub-cooling reduces the pump power required.

As the outlet temperature of the LNG heat exchanger increases, the cycle exergy destroyed to loss ratio and CERR decrease. As this temperature increases, most of the exergy destroyed shifts to the LNG heat exchanger and the overall exergy destroyed decreases because of a better match between the high temperature seawater and the propane stream. While this is favorable, the CERR decreases, meaning less exergy is taken from the stream and quality of exergy of the propane stream exiting the LNG heat exchanger decreases from a temperature of 117.5 K to 237.6 K. These values decrease when the mass flowrate is decreased. The cycle exergy destroyed to loss ratio and the CERR are depicted in Figure 6. Figure 7 shows the increasing stream match in the vaporizer for increases in the temperature.

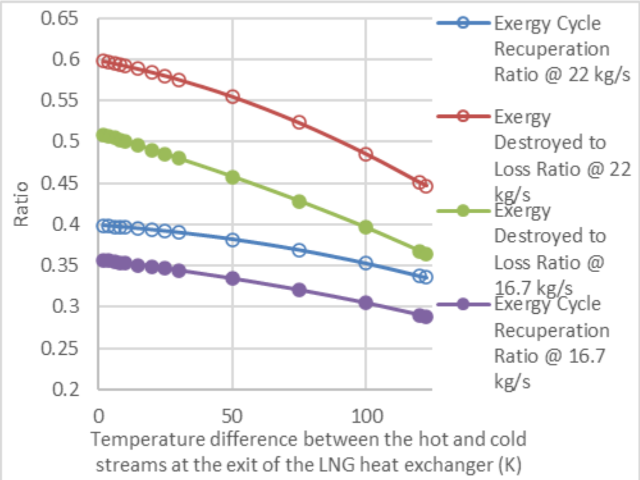

Figure 6 Ratio vs LNG Heat Exchanger Outlet Temperature Difference (Mass Flowrate: 22 kgs^{-1} & 16.7 kgs^{-1})

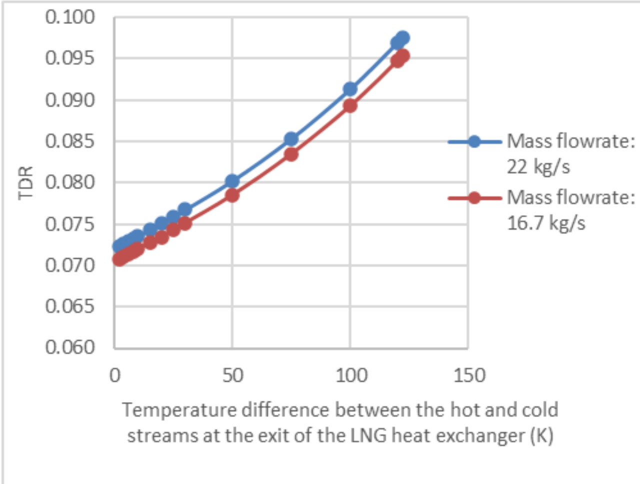

Figure 7 TDR vs Temperature Difference Between the Hot and Cold Streams at the Exit of the Vaporizer (K) at a dT_{min} = 2 K

The CEEE and the CEUE increase when the LNG heat exchanger outlet temperature difference increases. The heat load of the LNG heat exchanger and the vaporizer decrease resulting in the CEEE increase. The CEUE increases because the overall exergy destroyed decreases because of a better match between the hot and cold streams in the vaporizer. The CEUE increases for an increase in the mass flowrate while the CEEE does not change significantly. The CEEE and the CEUE at different mass flowrates are shown in Figure 8.

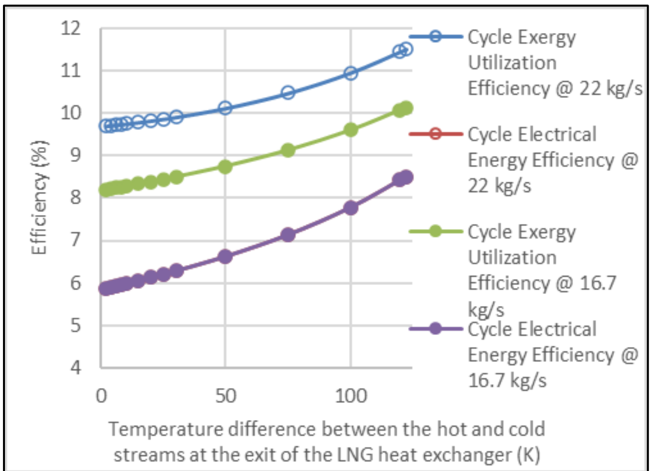

Figure 8 Efficiency vs LNG Heat Exchanger Outlet Temperature Difference (Mass Flowrate: 22 kgs^{-1} and 16.7 kgs^{-1})

Finally, an increase in the mass flowrate of the propane increases the power produced and the TAE until a pinch point is reached in the heat exchanger.

3.4. Propane Vaporizer Outlet Temperature Difference

The vaporizer is used to increase the energy of the propane stream. This energy is then extracted from the propane stream using the turboexpander. This section of the discussion evaluates the effect of the outlet temperature difference between the hot and cold stream on KPMs of the cycle.

An increase in the outlet temperature difference of the vaporizer decreases the power generated by the turboexpander. The enthalpy of the propane decreases as it approaches its dew / bubble point temperature. This was modelled using a linear model. A decrease in power generated causes a decrease in the TAE. Therefore, the more the propane is superheated the greater the earnings are. An increase of 1 K causes the TAE to decrease by USD5.1 k and this design has a potential maximum of USD305.2 k with an approach temperature of 1 K. This is shown in Figure 9:

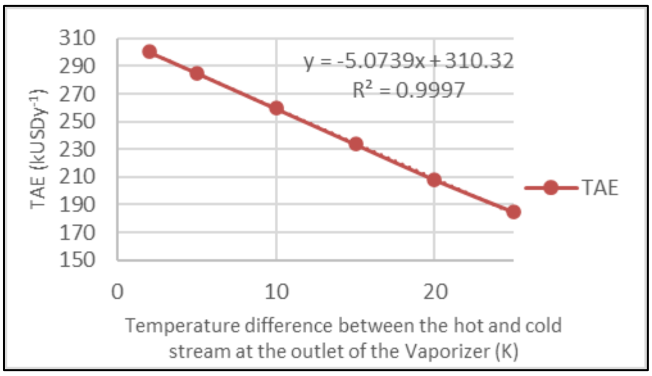

Figure 9 TAE vs Vaporizer Outlet Temperature Difference (Mass Flowrate: 22 kgs^{-1})

Increases in the outlet temperature difference of the vaporizer also decreases the CEEE and CEUE. This is mainly due to the decrease in power generated by the turboexpander while the duty of the vaporizer decreases. The CERR and the exergy ratio destroyed to loss also decrease for increases in the outlet temperature difference. An increase in the outlet temperature difference in the vaporizer results in more exergy destruction, it also results in the cold stream leaving the cycle with a higher work potential.

The power produced decreases as the propane outlet temperature and the heat load in the vaporizer decrease. The decrease results in a decrease in the area of the heat exchangers and an overall decrease in the AFCI and the TAE.

The outlet temperature difference in the vaporizer was then varied for different LNG heat exchanger outlet temperatures. It was found that the relationships above were still valid. That is as the outlet temperature difference in the vaporizer increases for different LNG heat exchanger outlet temperature differences the AFCI and TAE decrease.

3.5. Variation in the Turboexpander Inlet Pressure.

The turboexpander inlet pressure was then varied. The KPMs are evaluated in this section of the report by plotting them vs the turboexpander pressure ratio. The turboexpander outlet pressure was held constant in the simulation. The propane pump delivery pressure was increased which also increased the propane pump's motor power required.

The increase in turboexpander inlet pressure results in an increase in the power produced and hence AFCI and TAE. This is expected since the cost of the expander and generator increases with the power generated. The rate of increase reduces as the turboexpander inlet moves closer to its bubble / dew point pressure. The TDR also increases for the same minimum temperature difference as an increased heat capacity causes a better match between the hot and cold streams. Figure 10 to Figure 11 show the graph for TDR and TAE.

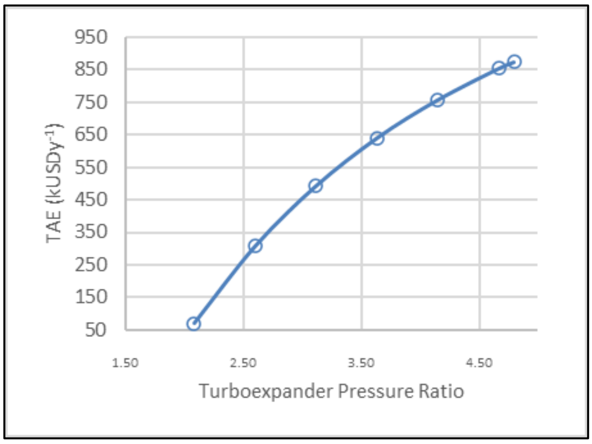

Figure 10 Power Produced vs Turboexpander Pressure Ratio

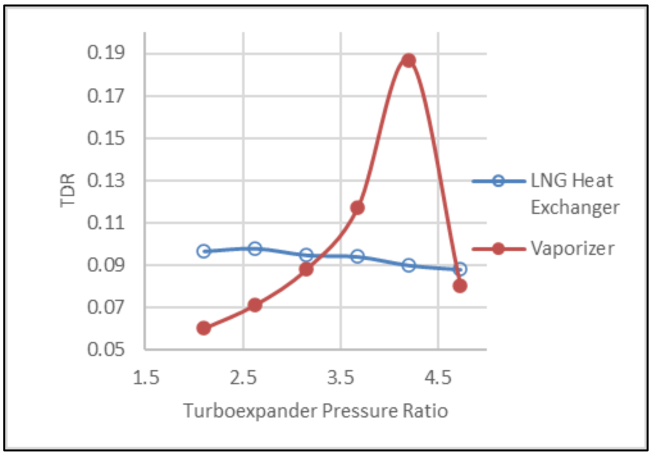

Figure 11 TDR vs Turboexpander Pressure Ratio

The overall effect on the cycle is an increase in the CEUE and the CEEE. A lower outlet temperature from the turboexpander was observed. The ratio of the exergy destroyed to loss and the CERR decrease. These findings are shown in Figure 12 and Figure 13:

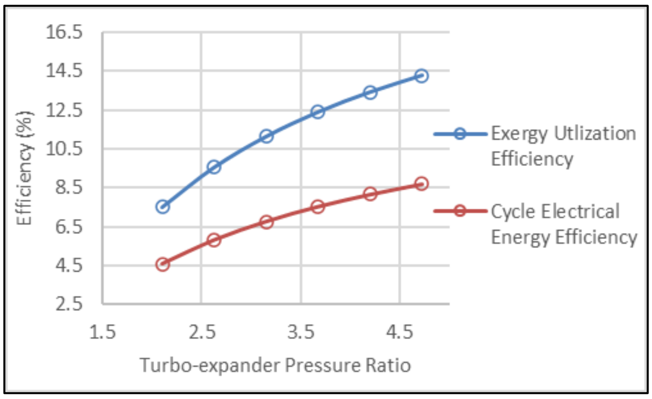

Figure 12 Efficiency vs Turboexpander Pressure Ratio

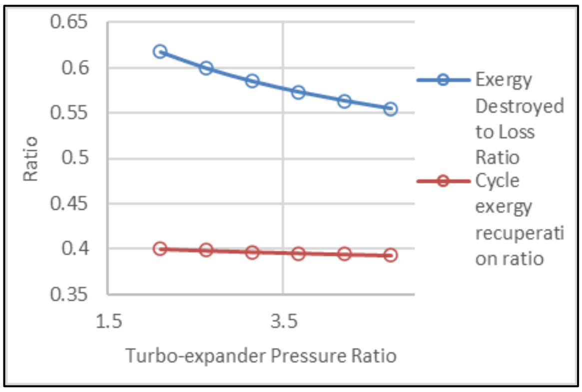

Figure 13 Ratio vs Turboexpander Pressure Ratio

3.6. Expander and Pump Efficiency

A sensitivity analysis was mainly conducted on the TAE to determine the equipment efficiencies that would make the project infeasible. It was simulated for pump efficiencies of 60 %, 70 % and 80 % and expander efficiencies of 70 %, 80 % and 90 % G. Towler et al [28] an R. Smith et al [39]. It is shown in Figure 14 that at an expander efficiency of more than 70 % and for all combinations of pump efficiencies, the project is feasible. A seawater pump efficiency of 80 % is required for the project to be feasible at an expander efficiency of 60 %. This is without flowrate optimization.

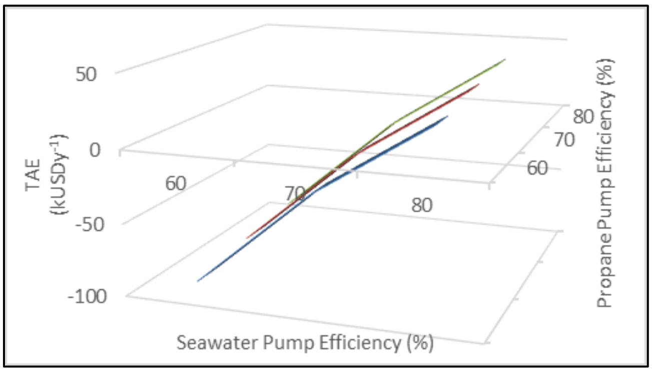

Figure 14 TAE vs Turboexpander and Pump Efficiencies

3.7. Electricity Price and the Interest Rate

An increase in the sale price causes the TAE to increase. An increase in the interest rate causes the AFCI to increase and the TAE to decrease. The electricity price and the interest rate at which the TAE changes to positive is shown in Figure 15. It shows that even at an interest rate of 8 % and an electricity cost of USD 0.15 per kWh the project is feasible.

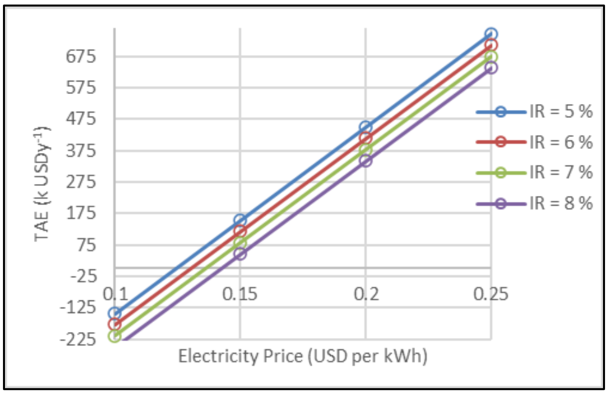

Figure 15 TAE vs Electricity Price for Different Tax Rates

3.8. LNG Pressure

As the LNG pressure increases the heat capacity of the LNG increases. This results in small increases in the AFCI and small decreases in the TAE. The CEUE and the CEEE increase while the exergy destroyed to exergy loss ratio and CERR decrease. Another important parameter the TDR increases at a constant minimum temperature difference in the LNG heat exchanger. Therefore, there is an opportunity to optimize the cycle by better matching the temperature profiles of the hot and cold streams by optimizing the propane mass flowrate. To operate the LNG at lower pressure, the ORC can be located at the end user. This may make pipeline transport of LNG feasible. It was found that at a mass flowrate of 26.4 kgs^{-1} (the LNG heat exchanger pinch point) and LNG pressure of 500 kPa_g the TAE and IRR were USD 535.9k and 18.5 %. This is an over 75% increase compared to LNG at 7 MPa_g. The TDR graph is shown below.

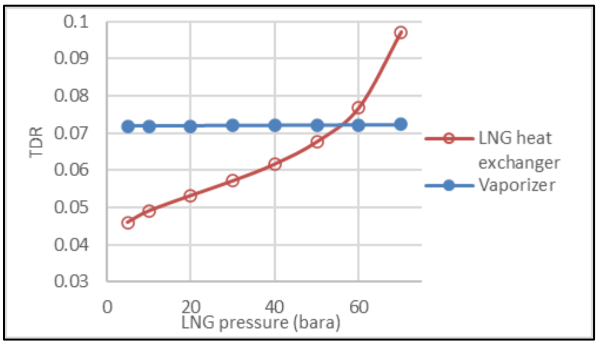

Figure 16 TDR vs LNG Pressure (bara)

4. Conclusion

The analysis above examines how different process parameters affect KPMs for the ORC. It also shows that the KPMs are good performance metrics of the cycle. The following are the findings of this analysis:1) The TAE and AIRR for the base case and alternate case are USD300.5k and 14 % and USD857.1k and 23.4 % respectively. These cases are therefore feasible; 2) the key process parameters are the turboexpander inlet pressure and temperature, LNG heat exchanger LNG inlet pressure and the outlet temperature difference and working fluid flowrate. There are several process variables that affect these process parameters. Increasing the turboexpander inlet pressure and temperature and the working fluid mass flowrate increase the turboexpander power output and the TAE. Increasing the LNG heat exchanger outlet temperature difference increases the TAE as it allows the working fluid mass flowrate to be optimized; 3) decreasing the LNG heat exchanger LNG inlet pressure allows the working fluid mass flowrate to be optimized. The new TAE and AIRR from the base case are USD535.9k and 18.5 % respectively for a LNG pressure of 500 kPa_g. These values are better than the base case values with the TAE being approximately 75 % more than the base case TAE. This has the potential to make the transport of LNG by pipeline feasible; 4) the analysis shows that the turboexpander accounts for over 70 % of the cost of the cycle and therefore decreasing the cost of the expander will directly impact the profitability of the cycle. It is concluded that this cold energy is an important source of energy and continued work in optimizing the recovery from this energy and in establishing the proper financial framework is important to maximize the gain from this energy source.

Compliance With Ethical Standards

Disclosure of conflict of interest

The author has no potential conflicts of interest to disclose

References

[1] "World Energy," [Online]. Available: https://www.iea.org/world/natural-gas. [Accessed 13 10 2025].

[2] "Assessing emissions from LNG supply and abatement options," [Online]. Available: https://www.iea.org/reports/assessing-emissions-from-lng-supply-and-abatement-options. [Accessed 13 10 2025].

[3] "Global natural gas demand growth set accelerate in 2026 as more LNG supply comes to market," International Energy Association, 22 07 2025. [Online]. Available: https://www,iea.org/news/global-natural-gas-demand-growth-set-to-accelerate-in-2026-as-more-lng-supply-comes-to-market. [Accessed 13 10 2025].

[4] "Shell LNG Outlook 2025," Shell, [Online]. Available: https://www.shell.com/what-we-do/oil-and-natural-gas/liquified-natural-gas-lng/lng-outlook-2025.html. [Accessed 14 10 2025].

[5] Y. Chen and X. Chen, "A technical analysis of heat exchangers in LNG plants and terminals," Natural Gas Industry, vol. 30, no. 1, pp. 96-100, 2010.

[6] G. Tagliafico, F. Valsuani and L. A. Tagliafico, "Liquified natural gas submerged combustion vaporization facilities: process integration with power conversion units," International Journal of Energy Research, vol. 37, no. 1, pp. 80-92, 2013, https://doi.org/10.1002/er.1937.

[7] F. Zihang, S. Kun and S. Tongwen, "Application of ambient air-based heating vaporizers in large LNG receiving terminals," Natural Gas industry, vol. 32, no. 8, pp. 100-4, 2012, https://doi.org/10.3787/j.issn.1000-0976.2012.08.022.

[8] R. F. Garcia, J. C. Carril, J. R. Gomez and M. R. Gomez, "Combined cascaded Rankine and direct expander based power units using LNG (liquified natural gas) cold as heat sink in LNG regasification," Energy, vol. 105, pp. 16-24, 2016, https://doi.org/10.1016/j.heliyon.2023e19393.

[9] H. Yu, X. Feng, Y. Wang, L. T. Biegler and J. Eason, "A systematic method to customize an efficient Organic Rankine Cycle (ORC) to recover waste heat in refineries," Applied Energy, vol. 179, pp. 302-15, 2016, https://doi.org/10.1016/j.apenergy.2016.06.093.

[10] D. Walraven, B. Laenen and W. D'Haeseleer, "Economic system optimization of air-cooled Organic Rankine Cycles (ORCs) powered by low-temperature geothermal heat sources," Energy, vol. 80, no. 0, pp. 104-13, 2015, https://doi.org/10.1016/j.energy.2014.11.048.

[11] Y. Jang and J. Lee, "Optimizations of the Organic Rankine Cycle (ORC) based domestic CHP using biomass fuel," Energy Conversion and Management, vol. 160, pp. 31-47, 2018, https://doi.org/10.1016/j.enconman.2018.01.025.

[12] T. Tartiere and M. Astolfi, "A world view of the organic rankine cycle market," Energy Procedia, vol. 129, pp. 2-9, 2017, https://doi.org/10.1016/j.egypro.2017.09.159.

[13] H. Yu, D. Kim and T. Gundersen, "A Study of Working Fluids for Organic Rankine Cycles Operating Across and Below Ambient Temperature to Utilize Liquefied Natural Gas (LNG Cold) Energy (Manuscript)," Energy, 2018, https://doi.org/10.1016/j.energy.2018.11.021.

[14] C. C. Yang and Z. Huang, "Lower emission LNG vaporization," LNG Journal, pp. 24-26, 2004.

[15] S. Yao, X. Shen, Z. Yang, G. Feng and M. Xiao, "Design and optimization of LNG vaporization cold energy comprenhensive utilization system based on a novel intermediate fluid vaporizer," Appl. Therm Eng, vol. 190, 2021, https://doi.org/10.1016/j.applthermaleng.2021.116785.

[16] H. Han, S. Wang, Y.-X. Li and Y. Yan, "Thermal design optimization analysis of an intermediate fluid vaporizer for liquefied natural gas," Appl. Therm Eng, vol. 129, pp. 329-337, 2018, https://doi.org/10.1016/j.applthermaleng.2017.10.043.

[17] C. E. Boyd, "Water temperature in aquaculture," Global seafood alliance, 26 11 2018. [Online]. Available: https://www.globalseafood.org/advocate/water-temperature-in-aquaculture/. [Accessed 15 10 2025].

[18] M. Akashah, N. Rozali and S. Mahadzir, "Utilization of Cold Energy from LNG Regasification Process: A Review of Current Trends," processes, vol. 11, 2023, https://doi.org/10.3990/pr11020517.

[19] A. Messineo and D. Panno, "Potential applications using LNG cold energy in Sicily," Int. J. Energy Res., vol. 32, no. 11, 2008, https://doi.org/10.1002/er.1411.

[20] M. Sermsuk, Y. Sukjai, M. Wiboonrat and K. Kiatkittipong, "Utilising Cold Energy from Liquefied Natural Gas to Reduce the Electricity Cost of Data Centres," energies, vol. 14, 2021, https://doi.org/10.3390/en14196269.

[21] S. B. A. Putra and M. Sudibandriyo, "Alternative of LNG cold exergy utilization for generating electrical energy at Gresik LNG receiving terminal," in Materials Science and Engineering, 2019, https://doi.org/10.1088/1757-899X/543/1/012044.

[22] A. M. Gerrard, "Guide to Capital Cost Estimating: Institution of Chemical Engineers," IChemE, 2000.

[23] J. Bao, R. Zhang, L. Y, N. Zhang, X. Zhang and G. He, "Simultaneous optimization of system structure and working fluid for the three stage condensation Rabkine cycle utilizing LNG cold energy," Applied Thermal Engineering, pp. 120-130, 2018, https://doi.org/10.1016/j.applthermaleng.2018.05.049.

[24] J. Park, L. I, F. You and I. Moon, "Economic Process Selection of Liquefied Natural Gas Regasification: Power Generation and Energy Storage Applications," Industrial & Engineering Chemistry Research, 2019, https://doi.org/10.1021/acs.iecr.9b00179.

[25] "Rayong Water Temperature," SeaTemperature.org, 17 10 2025. [Online]. Available: https://www.seatemperature.org/asia/thailand/rayong.htm. [Accessed 17 10 2025].

[26] T. Avetian and L. E. Rodriguez, "Fundamentals of turboexpander design and operation," Gas Processing and LNG, pp. 31-36, 2020.

[27] O. KoKu, S. Perry and J. Kim, "Techno-economic evaluation for the heat integration of vaporisation cold energy in natural gas processing," Applied Energy, vol. 114, pp. 250-261, 2014, http://dx.doi/10.1016/j.apenergy.2013.09.066.

[28] A. Laval, "The theory behind heat transfer (Plate heat exchangers)," 2004.

[29] C. Stenhede, "A Technical Reference Manual for Plate Heat Exchangers in Refrigeration & Air conditioning Applications," Alfa Laval AB, 2004.

[30] ALPEMA, The Standards of The Brazed Aluminium Plate-fin Heat Exchanger Manufacturers Association, 2014.

[31] G. Towler and R. Sinnott, Chemical Engineering Design (Principles, Practice and Economics of Plant and Process Design), Elsevier Inc., 2008.

[32] R. Smith, Chemical Process Design and Integration, West Sussex,: John Wiley & Sons, Ltd, 2016.

[33] R. Turton, R. Bailie, W. Whiting, J. Shaeiwitz and D. Bhattacharyya, Analysis, Synthesis, and Design of Chemical Processes, Upper Saddle River, New Jersey: Pearson Education International, 2013.

[34] C. Tammone, "Two-phase expansion in turbo-expanders for organic Rankine cycle power systems," Technical University of Denmark (DTU), Lyngby, 2023.

[35] C. Maxwell, "Cost Indicies," Towering Skills, 12 08 2025. [Online]. Available: https://toweringskills.com/financial-analysis/cost-indices/. [Accessed 21 10 2025].

[36] P. Gamonwet, S. Dhakal and K. Thammasiri, "The Impact of Renewable Energy Pricing Incentive Policies in Thailand," GMSARN International Journal, pp. 51-60, 2017.

[37] BoT, "Daily Foreign Exchange Rates," Bank of Thailand, [Online]. Available: https://www.bot.or.th/en/statistics/exchange-rate.html. [Accessed 5 9 2025].

[38] T. Economics, "Thailand Prime Lending Rate," Trading Economics, [Online]. Available: https://tradingeconomics.com/thailand/bank-lending-rate. [Accessed 5 9 2025].

[39] F. A. Holland, F. A. Watson and J. K. Wilkinson, Introduction to Process Economics, New York: John Wiley & Sons, 1983.

[40] "Economics Research Institute," Economics Research Institute, 4 9 2025. [Online]. Available: https://www.erieri.com/salary/job/process-operator/thailand#:~:text=The%20average%20pay%20for%20a,education%20for%20a%20Process%20Operator.. [Accessed 4 9 2025].

[41] J. W. Tester and M. Modell, Thermodynamics and It's Applications, 3rd ed., New Jersey: Prentice Hall, 1996.

[42] A. Atienza-Marquez, J. C. Bruno, A. Akisawa and A. Coronas, "Performance analysis of a combined cold and power (CCP) system with exergy recovery from LNG-regasification," Energy, vol. 183, pp. 448 - 461, 2019, https://doi.org/10.1016/j.energy.2019.06.153.

[43] A. Yasuo, "Power Generation Plant Using Cold in Osaka Gas," Osaka Gas Co. Ltd, Osaka-shi, 1983.

[44] M. Astolfi, "An Innovative Approach for the Techno-Economic Optimization of Organic Rankine Cycles," Politecnico Di Milano, Milan.